Enhanced magnetic flux concentration using windmill-like ferromagnets

Natanael Bort-Soldevila,[1, a)] Jaume Cunill-Subiranas,[1, a)] Aleix Barrera,[2] Nuria Del-Valle,[1] Alejandro V. Silhanek,[3] Vojtěch Uhlíř,[4,5] Simon Bending,[6] Anna Palau,[2] Carles Navau[1, b)]

[1)] *Departament de Física, Universitat Autònoma de Barcelona, 08193 Bellaterra, Barcelona, Spain*

[2)] *Institut de Ciència de Materials de Barcelona ICMAB-CSIC, Campus UAB, 08193 Bellaterra, Barcelona, Spain*

[3)] *Experimental Physics of Nanostructured Materials Q-MAT, CESAM, Université de Liège, B-4000 Sart Tilman, Belgium*

[4)] *CEITEC BUT, Brno University of Technology, Purkyňova 123, 612 00 Brno, Czechia*

[5)] *Institute of Physical Engineering, Brno University of Technology, Technická 2, 616 69 Brno, Czechia*

[6)] *Department of Physics, Centre for Nanoscience and Nanotechnology, University of Bath, BA2 7AY Bath, UK*

Magnetic sensors are used in many technologies and industries like medicine, telecommunication, robotics, the Internet of Things, etc. The sensitivity of these magnetic sensors is a key aspect, as it determines their precision. In this article, we investigate how a thin windmill-like ferromagnetic system can hugely concentrate a magnetic field at its core. A magnetic sensor combined with such a device enhances its sensitivity by a large factor. We describe the different effects that provide this enhancement: the thickness of the device and its unique windmill-like geometry. An expression for the magnetic field in its core is introduced and verified using finite-element calculations. The results show that a high magnetic field concentration is achieved for a low thickness-diameter ratio of the device. Proof-of-concept experiments further demonstrate the significant concentration of the magnetic field when the thickness-diameter ratio is low, reaching levels up to 150 times stronger than the applied field.

I. INTRODUCTION

Magnetic sensors are essential for numerous industries like telecommunication, medicine, automotive, aerospace, robotics, and consumer electronics to mention a few[1–9]. They make use of physical phenomena such as magnetoresistance[10], the Hall effect[11], or magnetic induction in order to measure the magnetic field. This gives information on the strength, direction, or proximity of the sensed magnetic field.

Sensitivity in these kinds of devices has a key role, as it determines the detection limit of the magnetic field and its precision. Highly precise and accurate sensors can be used to detect very weak magnetic fields. A great advantage for magnetic sensors is the possibility of their incorporation into a chip so that they need to be planar (2D). New emerging technologies, such as biomedical sensing[12] and the Internet of Things[13], stand to greatly benefit from on-chip devices with unprecedented field sensitivity.

The groundbreaking use of metamaterials has sparked a revolution in various research topics[14]. These artificially engineered materials possess effective properties not found in nature, enabling the manipulation of electromagnetic fields in extraordinary ways. Using the philosophy of transformation optics[15] it has been possible to design magnetic cloaks[16,17], hoses[18,19], wormholes[20], or devices capable of concentrating magnetic fields: magnetic concentrators[21,22]. However, while it is known that reducing the dimensionality of common magnetic materials (such as ferromagnets) directly affects their demagnetizing field[23,24], its influence on magnetic metamaterials is not so evident. Going beyond the limits of transformation-optics-related concentrators, their advantages could be combined with the magnetic properties arising when reducing the dimensions of ferromagnets. This would allow us to potentially obtain devices capable of enhancing the concentration of magnetic fields in order to improve the magnetic sensitivity for future sensors.

Although several designs have been proposed[25–29], in

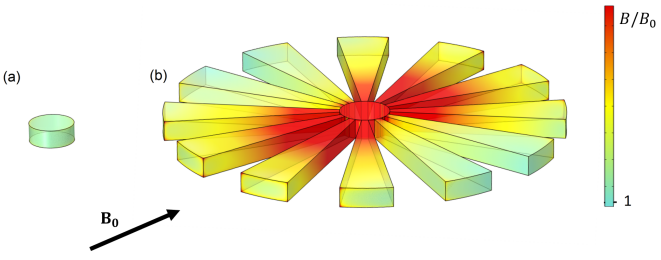

Figure 1. Generic representation of a concentration device comparing the magnetic field modulus B in (a) a bare ferromagnetic cylindrical core with (b) the same ferromagnetic core but with a shell of windmill blades, both exposed to the same uniform in-plane magnetic field, B_0. In this example, the relative permeability of the core was 100 and the red color indicates a factor $B/B_0 > 70$.

[a)] These two authors contributed equally to this work.
[b)] Electronic mail: carles.navau@uab.cat

this article, we study a windmill-like (also called flower-like in Ref. [22]) ferromagnetic device inspired by a magnetic concentrator metamaterial, which can be potentially used as an on-chip magnetic sensor.

II. THE WINDMILL-LIKE CONCENTRATOR

A. Description and model

The geometric design of the so-called concentrator employed in this paper is characterized by a small-thickness windmill-like pattern, consisting of a central ferromagnetic (FM) core and radial FM segments that symmetrically fan out, also called blades (or petals[22]). The blades have an inner radius R_1 (also the radius of the core), outer radius R_2, and thickness t. The design incorporates air gaps of the same size and shapes as the segments, strategically positioned between each segment. A graphical representation of such geometry is presented in Fig. 1b.

We also show in Fig. 1, numerical calculations of the magnetic field strength under an in-plane applied field considering that both the core and the blades are made of a linear, isotropic, and homogeneous material with relative permeability $\mu = 100$. We observe that the windmill-like device (Fig. 1b) significantly outperforms a bare FM core (Fig. 1a) in capturing the magnetic field. This means that by only adding the FM blades to the core we can achieve a large increase in the captured field at the core center, thus increasing the sensitivity of a magnetic sensor placed at the core.

In order to go into the details and give clues for the optimization of the windmill-like concentrators, we start by studying a large-thickness case. Consider an infinite cylindrical rod of a ferromagnet of radius R_2. The rod's long axis is aligned in the z direction, and a magnetic field is applied in the x direction. The magnetic field tends to concentrate in the interior of the FM rod homogeneously (shown in Fig 2a), distorting the outside field. The incremental factor of the magnetic field inside the rod is twice the applied field; since the demagnetizing factor for elliptical cylinders is $N_{m,r} = 1/2$,[23] *independent of the radius*. To further increase the field at the central axis of the cylinder one can use the transformation optics technique. Consider a ferromagnetic rod with radius R_1 and an anisotropic metamaterial shell of radius R_2 wrapped around it. The tensor permeability of the shell is given by a large radial permeability $\mu_r \to \infty$, and a low angular permeability $\mu_\theta \to 0$.[21] Using this shell, further concentration of the magnetic field is achieved at the FM core, as shown in Fig. 2b. This setup acts as the combination of the field concentrated with a 3D metamaterial shell and that of the cylindrical FM rod, giving a total field concentration of $2R_2/R_1$. When the FM rod is introduced at the center of the metamaterial shell, the magnetic field outside the concentrator becomes distorted, unlike the metamaterial shell without the inner

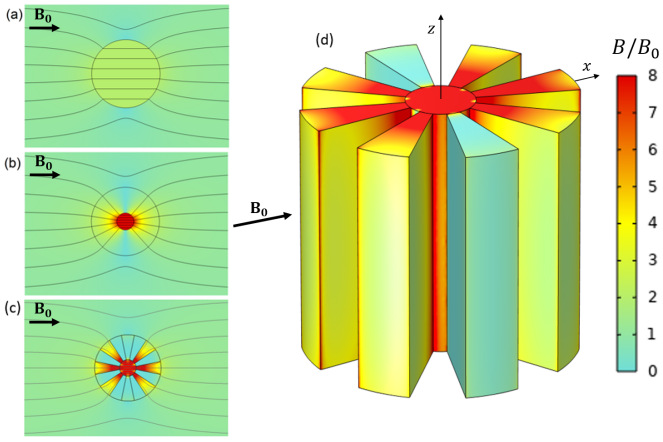

Figure 2. (a)-(c) Magnetic **B**-field modulus at an xy cross-sectional plane of an infinite (a) cylindrical FM core of radius R_2, (b) a cylindrical FM core of radius R_1 covered by an anisotropic material with large radial permeability, small angular permeability, and radius R_2, and (c) a cylindrical FM of radius R_1 with 8 FM blades which extend to a radius R_2. (d) 3D view of the magnetic **B**-field modulus of an arbitrary long portion of the (c) case.

FM core. This field outside the concentrator is distorted in exactly the same way as for a FM with a radius of R_2. This can be appreciated by comparing Figs. 2a and 2b.

A discretized, more realistic, and practical version of this metamaterial can be built by using a set of n linear, homogeneous, and isotropic (uniform permeability) FM blades around the inner FM core. The blades are separated by equally spaced air gaps. For example, considering $n = 8$ blades, as in Figs. 2c and 2d, closely mirrors the behavior of an ideal anisotropic shell, Fig. 2b.

For infinite concentrators, all xy cross-sectional planes are equivalent in terms of magnetic field. When the quotient R_2/R_1 is very large we can interpret the magnetic flux concentration as collecting the flux that threads a 2D surface into a 1D line; along the core of the concentrator (see Supplementary Material, section 2.1).

When considering finite cylinders/concentrators with a fixed thickness, new effects come into play. The symmetry along the z axis is lost, and the demagnetization effect in the z direction becomes relevant. For thin and homogeneous disks, demagnetizing factors ($N_{\mathrm{m,r}}$) that account for the radial magnetometric demagnetization have already been calculated for materials with any magnetic susceptibility χ.[30] The magnetic field strength inside thin disks can be expressed as

$$B = \frac{1+\chi}{1+N_{\mathrm{m,r}}\chi} B_0 \,. \tag{1}$$

The values of $N_{\mathrm{m,r}}$ are numerically calculated in Ref. [30] for several χ and thickness-to-diameter ratios, t/d.

For large values of χ, $N_{\mathrm{m,r}} < 1$ and decreases as t/d decreases. Thus, as t/d becomes smaller the magnetic field

Table I. Magnetic concentration factor B/B_0 at the center of the FM core for different $t/2R_2$ values). $R_2/R_1 = 4$. The simulated windmill-like concentrator has $\mu = 10^5$ and 8 blades.

$t/(2R_2)$	B/B_0 [Eq.(2)]	B/B_0 (windmill simul.)
0.013	363	292
0.050	83	84
1.188	28	31
∞	8.0	7.8

modulus inside the disk increases, always being larger than the applied field (Eq. (1)). Geometrically, we can understand the phenomenon as a decrease in the demagnetizing factor causing magnetic field lines from multiple parallel planes above and below the disk to converge toward the disk's interior. In other words, a small-thickness disk captures part of the field lines that would pass it above and below when incorporated in large-thickness cylinders.

A significant increase in the magnetic field can be achieved by leveraging both effects within a thin disk due to its demagnetization effect and the concentration of magnetic field lines in the center of the device using the FM core and blades. The combination of both strategies would first concentrate the field inside the disk (by the demagnetization effect) and then concentrate this field at the center of the device (through the FM blades). Combining both effects we could approximately express the field concentration at the core center as a function of the applied **B**-field (B_0) by

$$B \simeq \frac{R_2}{R_1}\frac{1+\chi}{1+N_{\mathrm{m,r}}\chi}B_0\,, \qquad (2)$$

if we assume that the demagnetization factor of a thin windmill-like geometry resembles that of a thin disk. In this expression, we consider that when the magnetic field lines get inside the concentrator, they are all funneled to the core center. The effectiveness of the R_2/R_1 term will depend on how well the shell is discretized; the more blades, the better (in the limiting ideal case of $n \to \infty$ and $\mu \to \infty$ the factor R_2/R_1 is exact). From Eq. (2) it is interesting to note that the smaller the thickness-diameter ratio is, the higher the field concentration would be at the core, as $N_{\mathrm{m,r}}$ tends to 0 when the thickness-to-diameter ratio tends to 0.

In Fig. 3 we show the results of the simulations for thickness with different thickness-to-diameter ratios (more results in Supplementary Material). Concentration values at the center of the inner core of the concentrator are in good agreement with the values predicted from Eq. (2) as shown in Table I. Even if the permeability of the material is not very high, high concentration is achieved (more details in the Supplementary Material).

This model is valid for linear, homogeneous, and isotropic (LHI) materials, with high magnetic permeabilities (mu-metal, permalloy, iron-nickel alloy) in a broad

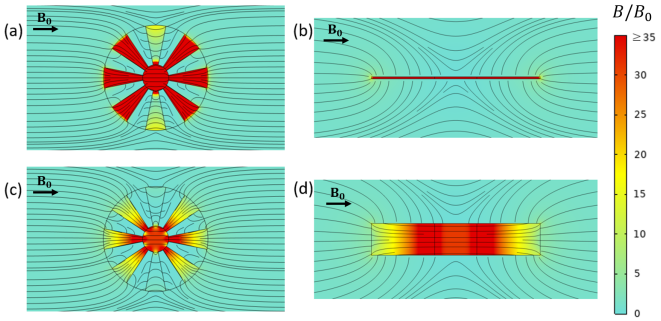

Figure 3. $|\mathbf{B}|$ for two different concentrators with different $t/(2R_2)$ ratios. Top: a concentrator with a $t/(2R_2) = 0.0025$ at (a) central plane and (b) $y = 0$ plane. Bottom: a concentrator with a $t/(2R_2) = 0.05$ at (c) central plane and (d) $y = 0$ plane. Notably, the concentrator with a smaller $t/(2R_2)$ ratio exhibits a greater field concentration.

range of magnetic fields. The concentration is thus limited by reaching the saturation of the material. It is essential to consider the scale of the concentrator, as it significantly affects its behavior. As the concentrator sizes and/or thickness-diameter ratios become small, the FM material ceases to behave as an LHI material. In such cases, magnetic domains can appear, and more sophisticated simulations have to be done (i. e. micromagnetics[22]), and Eq. (2) no longer works.

B. Proof-of-concept experiments

Proof-of-concept experiments were performed to verify the proposed model. In these experiments, samples of concentrators and disks with different thickness-diameter ratios were prepared by stacking mu-metal layers. The mu-metal concentrators used in the experiments had 8 blades and a ratio $R_2/R_1 = 4$, with a total diameter, $d = 2R_2$, of 8.25 cm. The diameter used for the mu-metal disks was the same as for the outer radius of the concentrators, $d = 8.25$ cm. In order to measure the magnetic field at the center of these geometries, a cut was made creating a gap of 1.0 mm in the concentrator/disk where a Hall probe was placed perpendicularly to the material plane. We used a Helmholtz coil pair to apply a uniform magnetic field B_0 of 0.2 mT in the plane of the device, perpendicular to the probe (we checked the linearity of the device up to applied fields of 1.9 mT). More details of the experimental measures are explained in Supplementary Material. In Fig. 4 we show images of the two different devices and plot a graph of the experimental field concentration as a function of t/d for both types of sample.

As expected, for low values of t/d the field concentration at the core increases up to a large factor. Using a concentrator we can achieve a field of more than 150 times the applied field, an outstanding concentration ratio. Also, it is important to note that for equivalent

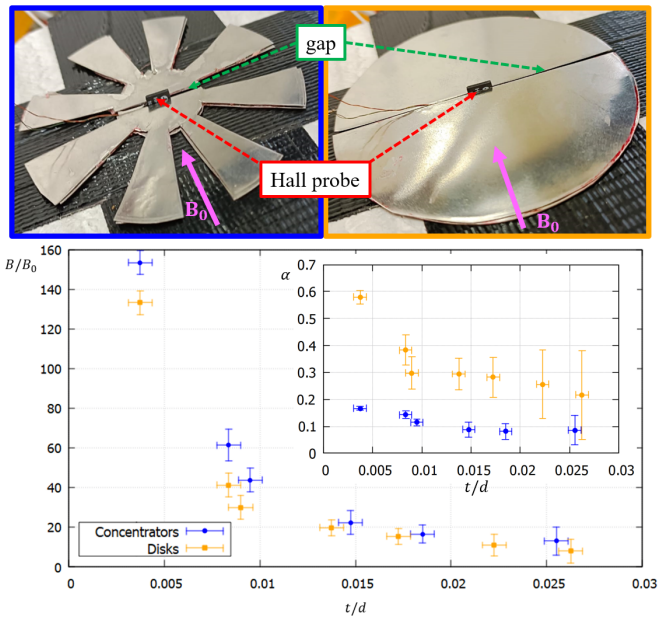

Figure 4. (Top) Photos of the two types of studied samples, concentrators with 8 blades (left) and disks (right). The Hall probe is placed in the center of the small gap and it is perpendicular to the plane of the device and to the applied field. (Bottom) Magnetic field concentration factor, B/B_0, as a function of the thickness-diameter ratio t/d of the sample. $B_0 = 0.2$ mT, $d = 4.25$ cm, and $R_2 = 4R_1$. Results are displayed for concentrators (in blue) and disks (in orange). In the inset, we plot the reduction factor due to the presence of the gap, α, as a function of t/d.

or similar t/d ratios, concentrators always have a higher concentration compared to the bare disks.

According to Eq. (2), one would expect a factor R_2/R_1 larger in the concentrators than the disks, which is not the case according to Fig. 4. This is because of the presence of the gap, which introduces a geometrical change in both, the concentrator and the disk. This gap alters the demagnetization factor in both samples, resulting in a different field value compared to that of a solid concentrator or disk at the core (Eqs. (2) and (1), respectively).

C. Discussion about the gap

In our experiment, the inclusion of the gap was necessary to measure the magnetic field at the center of the sample using a Hall probe. It is important to note that the gap must be a physical separation dividing the sample into two detachable parts, without contact between them. Otherwise, the field lines would pass through the FM bridge, and avoid passing through the Hall sensor. Additionally, the presence of the gap introduces anisotropy. The Hall probe detects the maximum magnetic field when the gap is oriented perpendicular to the applied magnetic field.

Numerical simulations of the samples with the gap reproduce the experimental measurements reasonably well, confirming that the presence of the gap is responsible for lowering the values of the magnetic concentration, compared to the theoretical gap-less devices (see details in Supplementary Material, Table S3). Then, the consideration of the gap introduces a correction factor in Eq. 2. This factor depends on the t/d ratio. In the inset of Fig. 4 we show a plot of an approximation of this factor, α, as a function of t/d, evaluated by dividing the simulated value of the concentration with the experimentally observed one. After this gap correction, the field at the core center as a function of the applied **B**-field, B_0, can be approximated by

$$B \simeq \alpha \frac{R_2}{R_1} \frac{1+\chi}{1+N_{\mathrm{m,r}}\chi} B_0. \tag{3}$$

Note that both α and $N_{\mathrm{m,r}}$ depend on t/d ($N_{\mathrm{m,r}}$ tabulated in Ref. [24] and α plotted in the inset of Fig. 4).

One possible way of avoiding this reduction of the field at the core is by filling the gap with another material, which should be used as a probe for magnetic fields, (in a similar way as done for giant magnetoresistance, planar Hall effect, or Pole Barber based sensors[31–34], for example). This means that there must be no space with air between the high permeability material of the sample and this probe material. Moreover, this permeability should be as high as possible to obtain the greatest concentration. Numerical simulations also have been performed to show how filling the gap with another material of different permeability affects the concentration (see Table S4 in the Supplementary Material). The addition of this material clearly indicates an increment of the concentration field. Moreover, the higher the permeability in the gap, the closer the concentration approaches the theoretical values.

III. CONCLUSIONS

To conclude, by combining the ideas of magnetic metamaterials, the effects of the windmill-like concentrators, and the demagnetizing fields in finite geometries, we have demonstrated the achievement of unprecedented field concentrations in a planar device capable of being built on-chip. This could be useful for many technologies where magnetic sensors are present. Beyond sensors, the use of such devices for changing some effective properties (coercivity, ...) could be also explored. An expression describing the combination of all these effects was proposed and validated through numerical analysis. Proof-of-concept experiments showcased the remarkably high levels of magnetic field concentration attainable in such a windmill-like system. Even though further calculations including magnetic domains and micromagnetics ought to be performed to find how these systems behave at extremely thin limits and/or microsized concentrators, our approach is always valid for LHI materials.

DESCRIPTION OF THE SUPPLEMENTARY MATERIAL

Details of the numerical simulations performed, as well as a detailed description of the experimental procedure. Complementary information containing discussion on the dimensions, thickness, permeability, and the gap effects on the results.

ACKNOWLEDGMENTS

This work was supported by (a) Spanish Ministry of Science and Innovation MCIN/ AEI /10.13039/501100011033/ through CHIST-ERA PCI2021-122028-2A, PCI2021-122083-2A (co-financed by the European Union Next Generation EU/PRTR), HTSUPERFUN PID2021-124680OB-I00 (cofinanced by ERDF "A way of making Europe"), PID2019-104670GB-I00; (b) Fonds de la Recherche Scientifique - FNRS under the programs PDR T.0204.21, CDR J.0176.22, and EraNet-CHIST-ERA R.8003.21 (c) The Research Foundation and by European Cooperation in Science and Technology (COST, www.cost.eu) through COST Action SUPERQUMAP (CA 21144); (d) TACR EraNet CHIST-ERA project MetaMagIC TH77010001; and (e) Engineering and Physical Sciences Research Council (EPSRC) in the United Kingdom under Grant No. EP/W022680/1. J. C.-S. acknowledges funding from AGAUR-FI Joan Oró grants (2023 FI-3 00065), Generalitat de Catalunya. A. B. acknowledges support from MICIN Predoctoral Fellowship (PRE2019-09781) and UAB doctorate program on Materials Science.

AUTHOR DECLARATIONS

COI statement

The authors have no conflicts to disclose.

CRediT statement

Natanael Bort-Soldevila: idea of the study, design of the experiments (lead), performing experiments (lead), numerical simulations, analysis, original draft (lead), review. **Jaume Cunill-Subiranas**: idea of the study, design of the experiments (lead), performing experiments (lead), numerical simulations (lead), analysis, original draft, review. **Aleix Barrera**: design of the experiments (support), analysis, review. **Nuria Del-Valle**: idea of the study, analysis, review. **Alejandro V. Silhanek**: idea of the study, analysis, review, funding acquisition. **Vojtěch Uhlíř**: idea of the study, analysis, review, funding acquisition. **Simon Bending**: idea of the study, analysis, review, funding acquisition. **Anna Palau**: idea of the study, design of the experiments (support), analysis, review, funding acquisition. **Carles Navau**: idea of the study, analysis, original draft, review (lead), funding acquisition, general supervision.

REFERENCES

[1] P. Ripka and M. Arafat, "Magnetic sensors: Principles and applications," in *Reference Module in Materials Science and Materials Engineering* (Elsevier, 2019).
[2] J. Heremans, "Solid-state magnetic-field sensors and applications," Journal of Physics D-Applied Physics **26**, 1149–1168 (1993).
[3] D. Murzin, D. J. Mapps, K. Levada, V. Belyaev, A. Omelyanchik, L. Panina, and V. Rodionova, "Ultrasensitive magnetic field sensors for biomedical applications," SENSORS **20** (2020), 10.3390/s20061569.
[4] A. Sobczak-Kupiec, J. Venkatesan, A. A. AlAnezi, D. Walczyk, A. Farooqi, D. Malina, S. H. Hosseini, and B. Tyliszczak, "Magnetic nanomaterials and sensors for biological detection," Nanomedicine-Nanotechnology Biology and medicine **12**, 2459–2473 (2016).
[5] M. Diaz-Michelena, "Small magnetic sensors for space applications," SENSORS **9**, 2271–2288 (2009).
[6] L. Pan, Y. Xie, H. Yang, M. Li, X. Bao, J. Shang, and R.-W. Li, "Flexible magnetic sensors," Sensors **23** (2023), 10.3390/s23084083.
[7] I. Koh and L. Josephson, "Magnetic nanoparticle sensors," SENSORS **9**, 8130–8145 (2009).
[8] J. Lenz, "A review of magnetic sensors," Proceedings of the IEEE **78**, 973–989 (1990).
[9] C. P. Gooneratne, B. Li, and T. E. Moellendick, "Downhole applications of magnetic sensors," Sensors **17** (2017), 10.3390/s17102384.
[10] C. Zheng, K. Zhu, S. Cardoso de Freitas, J.-Y. Chang, J. E. Davies, P. Eames, P. P. Freitas, O. Kazakova, C. Kim, C.-W. Leung, S.-H. Liou, A. Ognev, S. N. Piramanayagam, P. Ripka, A. Samardak, K.-H. Shin, S.-Y. Tong, M.-J. Tung, S. X. Wang, S. Xue, X. Yin, and P. W. T. Pong, "Magnetoresistive sensor development roadmap (non-recording applications)," IEEE Transactions on Magnetics **55**, 1–30 (2019).
[11] E. Ramsden, "Hall-effect sensors : theory and applications," (2006).
[12] O. G. S. G. Lin, D. Makarov, "Magnetic sensing platform technologies for biomedical applications," Lab on a chip **17**, 1884 (2017).
[13] M. A. Khan, J. Sun, B. Li, A. Przybysz, and J. Kosel, "Magnetic sensors-a review and recent technologies," Engineering Research Express **3**, 022005 (2021).
[14] M. Kadic, G. W. Milton, M. van Hecke, and M. Wegener, "3d metamaterials," Nature Reviews Physics **1**, 198–210 (2019).
[15] J. B. Pendry, A. Aubry, D. R. Smith, and S. A. Maier, "Transformation optics and subwavelength control of light," Science **337**, 549–552 (2012), https://www.science.org/doi/pdf/10.1126/science.1220600.
[16] F. Gömöry, M. Solovyov, J. Souc, C. Navau, J. Prat-Camps, and A. Sanchez, "Experimental realization of a magnetic cloak," Science **335**, 1466–1468 (2012), https://www.science.org/doi/pdf/10.1126/science.1218316.
[17] S. Narayana and Y. Sato, "Dc magnetic cloak," Advanced Materials **24**, 71–74 (2012).
[18] C. Navau, J. Prat-Camps, O. Romero-Isart, J. I. Cirac, and A. Sanchez, "Long-distance transfer and routing of static magnetic fields," Phys. Rev. Lett. **112**, 253901 (2014).
[19] P. Zhou, G. Ma, H. Liu, X. Li, H. Zhang, C. Yang, and C. Ye, "Transportation of static magnetic fields by a practically realizable magnetic hose," IEEE Magnetics Letters **7**, 1–4 (2016).
[20] J. Prat-Camps, C. Navau, and A. Sanchez, "A magnetic wormhole," Scientific Reports **5**, 12488 (2015).

[21]C. Navau, J. Prat-Camps, and A. Sanchez, "Magnetic energy harvesting and concentration at a distance by transformation optics," Phys. Rev. Lett. **109**, 263903 (2012).
[22]E. Fourneau, J. A. Arregi, A. Barrera, N. D. Nguyen, S. Bending, A. Sanchez, V. Uhlíř, A. Palau, and A. V. Silhanek, "Microscale metasurfaces for on-chip magnetic flux concentration," Advanced Materials Technologies **8**, 2300177 (2023).
[23]J. A. Osborn, "Demagnetizing Factors of the General Ellipsoid," Physical Review **67**, 351–357 (1945).
[24]D.-X. Chen, J. Brug, and R. Goldfarb, "Demagnetizing factors for cylinders," IEEE Transactions on Magnetics **27**, 3601–3619 (1991).
[25]A. S. Edelstein, G. A. Fischer, M. Pedersen, E. R. Nowak, S. F. Cheng, and C. A. Nordman, "Progress toward a thousandfold reduction in $1/f$ noise in magnetic sensors using an ac microelectromechanical system flux concentrator," Journal of Applied Physics **99**, 08B317 (2006).
[26]X. Sun, L. Jiang, and P. W. Pong, "Magnetic flux concentration at micrometer scale," Microelectronic Engineering **111**, 77–81 (2013).
[27]P. M. Drljača, F. Vincent, P.-A. Besse, and R. S. Popović, "Design of planar magnetic concentrators for high sensitivity hall devices," Sensors and Actuators A: Physical **97-98**, 10–14 (2002), selected papers from Eurosenors XV.
[28]W. C. Griffith, R. Jimenez-Martinez, V. Shah, S. Knappe, and J. Kitching, "Miniature atomic magnetometer integrated with flux concentrators," Applied Physics Letters **94**, 023502 (2009).
[29]X. Sun, L. Jiang, and P. W. Pong, "Magnetic flux concentration at micrometer scale," Microelectronic Engineering **111**, 77–81 (2013).
[30]D.-X. Chen, E. Pardo, and A. Sanchez, "Radial magnetometric demagnetizing factor of thin disks," IEEE Transactions on Magnetics **37**, 3877–3880 (2001).
[31]P. D. Kulkarni, H. Iwasaki, and T. Nakatani, "The effect of geometrical overlap between giant magnetoresistance sensor and magnetic flux concentrators: A novel comb-shaped sensor for improved sensitivity," Sensors **22** (2022), 10.3390/s22239385.
[32]S. Uchaikin and H. Sanghera, "Low field magnetic sensing with anisotropic magnetoresistive sensors," (2013).
[33]M. Volmer and J. Neamtu, "Micromagnetic analysis and development of high sensitivity spin-valve magnetic sensors," Journal of Physics: Conference Series **268**, 012032 (2011).
[34]A. Grosz, V. Mor, E. Paperno, S. Amrusi, I. Faivinov, M. Schultz, and L. Klein, "Planar hall effect sensors with subnanotesla resolution," IEEE Magnetics Letters **4**, 6500104–6500104 (2013).